

On faults in the framework structure of the zeolite ferrierite

R. Gramlich-Meier, W. M. Meier and B. K. Smith¹

Institute of Crystallography and Petrography, ETH, CH-8092 Zürich, Switzerland

Received: June 28, 1984

Ferrierite / Zeolites / Structural faults

Abstract. The crystal structure of ferrierite ($\text{Na}_{0.2}\text{K}_{0.8}\text{Ca}_{0.5}\text{Mg}_2$) $\text{Al}_7\text{Si}_{29}\text{O}_{72}$ $18\text{H}_2\text{O}$ was reexamined using X-ray diffractometer data. This refinement confirmed the orthorhombic structure of Vaughan. According to electron diffraction analyses of ferrierites from three localities most crystals show no deviation from the *Immm* structure. However, several diffraction patterns were found to exhibit streaking parallel to $[010]^*$ and $[110]^*$. Models of conservative and non-conservative faults were derived which could account for these diffraction patterns.

Introduction

The crystal structure of ferrierite (ideal composition $\text{Na}_2\text{Mg}_2\text{Al}_6\text{Si}_{30}\text{O}_{72}$ $\sim 18\text{H}_2\text{O}$) was first determined by Vaughan (1966). It can be classified unambiguously as a member of the mordenite family of zeolite structures based on 5–1 secondary building units (Meier, 1968). A 3-dimensional skeletal diagram of the aluminosilicate framework of ferrierite is shown in Figure 1 and a schematic projection along the *c* axis is presented in Figure 2. The framework structure, in which 5-rings abound, is traversed by channels along $[001]$ with oval 10-ring openings. These main channels intersect with side channels parallel to $[010]$ with apertures formed by 8-ring openings. Ferrierite-type materials have noteworthy molecular sieve properties which are due to the 2-dimensional intersecting channel system.

The maximum topological symmetry of the ferrierite framework structure is *Immm* and this space group is generally observed by X-ray diffraction. Vaughan (1966) recorded no deviation from this symmetry in his structure refinement based on film data though lower symmetry was considered as a

¹ Present address: Department of Geology, Arizona State University, Tempe, AZ 85287

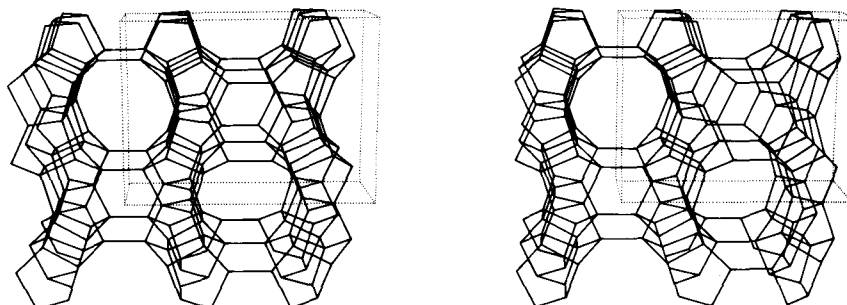


Fig. 1. Stereo-pair of the skeletal framework of ferrierite viewed along [001]

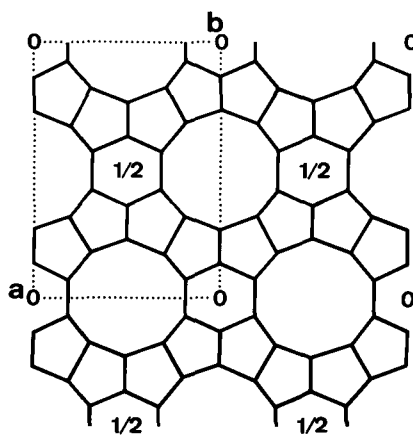


Fig. 2. Schematic structure of ferrierite in projection along c

possibility in his discussion of the results. Symmetry lower than $Immm$ is indeed not only indicated by a stretched $T-O-T$ ($T=Si, Al$) bridge at $O(5)$, but even more so by the fact that any reasonable Si, Al -ordering scheme is incompatible with $Immm$ symmetry.

In this paper an X-ray examination of the crystal structures of ferrierite is presented, followed by a discussion of structural faults based on electron diffraction data.

X-ray structure analysis

A crystal from Silver Mountain, California (kindly supplied by Mr. R. Tschernich) was used to verify the crystal structure determined by Vaughan (1966). The chemical composition for this crystal is $(Na_{0.2}K_{0.8}Ca_{0.5}Mg_2)$

$\text{Al}_7\text{Si}_{29}\text{O}_{72} \cdot 18\text{H}_2\text{O}$ (from Wise and Tschernich, 1976). X-ray precession and Weissenberg photographs confirmed the lattice constants and the extinction condition $h+k+l=2n$. Refined values for the lattice constants ($a=19.220(11)$, $b=14.124(9)$, $c=7.493(5)$ Å) were obtained from 30 reflections centered automatically on a Picker FACS-1 diffractometer using monochromatic $\text{MoK}\alpha$ radiation.

In the region $2\theta < 60^\circ$ of the reciprocal space, 1705 independent reflections were measured (with $h+k+l=2n$), of which 726 were observed with $I > 3\sigma(I)$. No absorption correction was applied. The refinement was started using the structural parameters given by Vaughan (1966), with *T* sites refined using neutral Si scattering factors. The least-squares refinement converged to a conventional *R* value of 0.072 for the observed reflections. Final atom coordinates and anisotropic temperature factors are listed in Table 1¹. No unusually large temperature factors were observed.

No pronounced deviations from the crystal structure determined by Vaughan were noted. The interatomic distances (Table 2) are rather short, also in agreement with Vaughan's results. Except for Mg and atom position IV, which is most likely Na or K, the remaining non-framework sites (I–VII) can probably be assigned to water molecules. The Mg^{2+} ion is octahedrally coordinated by water molecules labelled as sites I, II, and III. The Mg– H_2O distances are 2.00(1), 2.12(1) and 2.12(1) Å for sites I, II, and III, respectively. The orientation of the $\text{Mg}(\text{H}_2\text{O})_6^{2+}$ octahedra disobeys the site symmetry *mmm* thus giving rise to apparent disorder as described by Vaughan.

A rare occurrence (at the Altoona locality, Washington, USA) of low Mg ferrierite with unusual diamond shaped habit was described by Wise and Tschernich (1976). Its monoclinic structure was refined by Gramlich-Meier et al. (submitted). This highly uncommon variety of ferrierite is not dealt with in the present work.

Electron diffraction

Experimental

Typical ferrierites from three sample localities were chosen for the TEM study. The locations and samples from Silver Mountain (California) and from Altoona (Washington) have been described in detail by Wise and Tschernich (1976). The 'Altoona' crystals examined in the present study correspond to their lath-shaped Altoona 2 samples. Ferrierite from the third locality, Lovelock (Nevada), was chosen due to its unique occurrence in a sedimentary environment (Regis, 1970; Sheppard and Gude, 1983).

¹ Additional material to this paper can be ordered referring to the no. CSC 51092, name(s) of the author(s) and citation of the paper at the Fachinformationszentrum Energie Physik Mathematik, D-7514 Eggenstein-Leopoldshafen 2, FRG

Table 1. Atom coordinates and thermal parameters

Atom	PP	x	y	z	U_{11}^{**}	U_{22}	U_{33}	U_{12}	U_{13}	U_{23}
T(1)	*	0.1552(2)	0	0	0.012(2)	0.009(2)	0.019(3)	0	0	0
T(2)		0.0843(2)	0.2031(3)	0	0.008(1)	0.014(1)	0.013(2)	0.000(1)	0	0
T(3)		0.2718(2)	0	0.2920(6)	0.023(2)	0.013(1)	0.016(2)	0	-0.007(2)	0
T(4)		0.3229(1)	0.2024(2)	0.2072(3)	0.0163(9)	0.0150(9)	0.013(1)	-0.0012(9)	-0.0015(9)	-0.001(1)
O(1)		0	0.216(1)	0	0.001(4)	0.036(9)	0.04(1)	0	0	0
O(2)		0.249(1)	0	0.5000	0.044(9)	0.035(9)	0.019(8)	0	0	0
O(3)		0.1020(6)	0.0901(9)	0	0.032(6)	0.021(5)	0.10(1)	0.006(5)	0	0
O(4)		0.2021(7)	0	0.179(2)	0.032(6)	0.11(1)	0.023(8)	0	-0.016(5)	0
O(5)		0.2500	0.2500	0.2500	0.038(5)	0.040(7)	0.06(1)	0.022(5)	0.001(7)	-0.008(7)
O(6)		0.3428(8)	0.220(1)	0	0.056(7)	0.052(8)	0.014(5)	-0.005(6)	0	0
O(7)		0.1157(4)	0.2501(8)	0.182(1)	0.035(4)	0.066(6)	0.038(7)	-0.008(4)	-0.016(4)	-0.029(5)
O(8)		0.3211(5)	0.0914(6)	0.248(1)	0.053(5)	0.019(3)	0.058(7)	0.003(4)	0.010(6)	0.015(4)
Mg		0	0	0.5000	0.016(4)	0.036(6)	0.030(6)	0	0	0
I	1.00	0	0	0.233(2)	0.026(7)	0.05(1)	0.014(8)	0	0	0
II	0.40	0.403(1)	0.429(3)	0	0.03(1)	0.04(2)	0.02(1)	-0.02(1)	0	0
III	0.67	0.450(3)	0.366(3)	0	0.21(4)	0.07(2)	0.06(2)	-0.07(3)	0	0
IV	1.06	0.4286(6)	0	0	0.009(6)	0.018(6)	0.034(8)	0	0	0
V	0.32	0.440(3)	0	0.23(1)	0.08(3)	0.03(3)	0.12(5)	0	0.03(4)	0
VI	0.76	0.5000	0.126(7)	0.20(1)	0.04(1)	0.5(1)	0.5(1)	0	0	-0.3(1)
VII	0.5	0.38(1)	0.5000	0	0.3(2)	0.2(1)	0.3(3)	0	0	0

* Population parameters are given for the non-framework atoms I–VII only and are referred to neutral oxygen. Estimated standard deviations are 0.05.

** Form of the anisotropic temperature factor:

$$\exp [-2(\pi^2)\{U_{11}(h^2)(a^*)^2 + \dots + 2U_{23}k lb^* c^*\}]$$

Table 2. Interatomic distances and bond angles of the aluminosilicate framework

<i>T-O distances</i>			
T(1)-O(3) (× 2)	1.63(2) Å	T(2)-O(1)	1.63(2) Å
T(1)-O(4) (× 2)	1.62(2)	T(2)-O(3)	1.63(2)
Mean	1.63	T(2)-O(7) (× 2)	1.63(1)
		Mean	1.63
T(3)-O(2)	1.62(1) Å	T(4)-O(5)	1.59(1) Å
T(3)-O(4)	1.58(2)	T(4)-O(6)	1.62(1)
T(3)-O(8) (× 2)	1.63(2)	T(4)-O(7)	1.59(2)
Mean	1.62	T(4)-O(8)	1.60(1)
		Mean	1.60
<i>O-T-O angles*</i>			
O(3)-T(1)-O(4) (× 4)	110°	O(1)-T(2)-O(3)	108°
O(3)-T(1)-O(3)'	102	O(1)-T(2)-O(7) (× 2)	109
O(4)-T(1)-O(4)'	112	O(3)-T(2)-O(7) (× 2)	109
		O(7)-T(2)-O(7)'	113
O(2)-T(3)-O(4)	107°	O(5)-T(4)-O(6)	110°
O(2)-T(3)-O(8) (× 2)	111	O(5)-T(4)-O(7)	112
O(4)-T(3)-O(8) (× 2)	112	O(5)-T(4)-O(8)	111
O(8)-T(3)-O(8)'	104	O(6)-T(4)-O(7)	105
		O(6)-T(4)-O(8)	110
		O(7)-T(4)-O(8)	109
<i>T-O-T angles*</i>			
T(2)-O(1)-T(2)'	167°	T(4)-O(5)-T(4)'	180°
T(3)-O(2)-T(3)'	149	T(4)-O(6)-T(4)'	147
T(1)-O(3)-T(2)	153	T(2)-O(7)-T(4)	152
T(1)-O(4)-T(3)	156	T(3)-O(8)-T(4)	146

* Estimated standard deviations of 0.8 and 1.0 degrees for the O-T-O and T-O-T angles respectively

Samples were prepared for TEM analysis following essentially the method 1 of Cartlidge et al. (1983). In brief, clusters of ferrierite crystals were hand-picked from the host rock and gently ground in a mortar. This powder was then suspended in anhydrous ethanol, and the suspension was dropped by pipette on 3mm copper grids covered with a holey carbon film. Most of the crystallites on the carbon film lay on the predominant (100) or (010) faces, but use of a high angle double tilting stage ($\pm 45^\circ$) permitted a variety of orientations to be obtained.

The principal limitation in using TEM to study zeolites is the propensity of these minerals to vitrify within seconds under normal illumination conditions. Although several specimen treatments have been proposed to extend the 'lifetime' of irradiated zeolites, (Bursill et al., 1981, Hirsch (discussion and reply), 1981), recent TEM work with zeolites has been

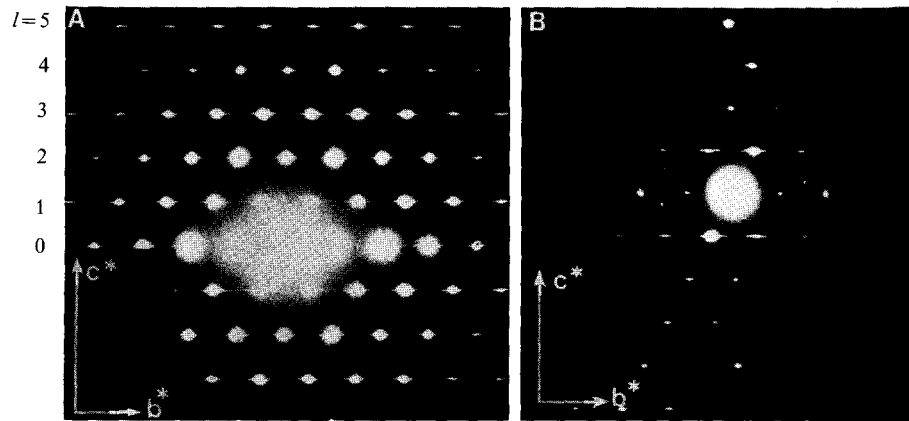


Fig. 3. SAD's of incommensurate structures. a): continuously streaked reflections superimposed on the *Immm* pattern parallel to b^* . Lovelock. b): continuously streaked b^* reflections, with pronounced streaking on the l odd rows and very little streaking on l even. Altoona

successfully completed by using techniques to minimize the electron flux through an untreated specimen (Thomas et al., 1983). We considered these latter procedures to be preferable as one can examine the original crystal structure without any possible modifications which may be introduced by pre-treatment.

In practise, we prolonged the stability of the ferrierite crystals by using a highly decondensed beam, and by translating any given grain well outside of the beam diameter during focussing or alignment corrections. Use of such a decondensed beam necessarily requires an attendant increase in exposure time for micrographs, which limited the number of orientations that one could sample and precluded the ability to conduct rigorous 2-beam analysis of defects. Further, the low electron flux limits the penetration thickness of the beam to only the thinnest areas of a given crystallite. It was noted, however, that the lifetime of the ferrierite crystals increased enormously with increasing voltage: crystals maintained their integrity for roughly 3 times longer at 200 kV compared to 100 kV.

Observations

As the subgrain diameters are of the order of 2000 Å electron diffraction patterns (SAD patterns) were obtained using the smallest selected area ('intermediate') apertures (projected diameter of 6000 Å for 20 micron aperture).

Occasional deviations from the *Immm* symmetry were observed within the limited probe cross-sections. It must be stressed, however, that the large

majority of ferrierite grains from all three localities did *not* display any detectable deviations from this higher symmetry. This may reflect in some degree the experimental conditions used: SAD patterns taken at 200 kV displayed more evidence of streaking and extra reflections than those taken at 100 kV, presumably due to the greater penetration and sample volumes that are obtainable at higher voltages.

The most common feature of the diffraction patterns is streaking of the diffraction spots in the b^* direction (Fig. 3a and b). In $0kl$ SAD patterns of crystals containing these defects, the streaking is often continuous between the diffraction spots, with no clear subsidiary maxima along the streak nor any discernable difference in streak intensity between the l even or l odd rows of points. However, it is also typical to find well pronounced streaks on only the l odd rows, with little or no elongation of the diffraction spots parallel to b^* on the l even rows (Fig. 3b). Several occurrences of discontinuous streaks were also noted parallel to the $[110]^*$ direction, but these are not so common.

Discussion

Streaking as observed in the electron diffraction patterns of ferrierite (Fig. 3) must be due to essentially 2-dimensional faults. Such faults separate regions which are related by translations different from lattice vectors.

Likely fault planes can be found readily in the framework structures of mordenite and many other zeolites (cf. Sherman and Bennett, 1973; Meier and Olson, 1978). On the other hand, no such shear planes giving rise to stacking faults and polytypism can be located in the ferrierite type framework.

A very useful conceptual device for elucidating possible faults is the sigma transformation as first introduced by Shoemaker, Robson and Broussard (1973) to correlate various framework structures. A sigma plane in a tetrahedral framework can but need not be a crystallographic mirror plane. It is a planar or near-planar arrangement of $(-T-O)_n$ chains or rings with linking oxygen atoms on both sides of the plane in opposite positions. No other framework atoms are allowed in the plane nor may T-O bonds intersect a sigma plane. The contents of a sigma plane can be doubled leading to double chains or double rings (sigma transformation) subject to angular constraints.

The ferrierite framework contains sigma planes parallel to (010) and (110) as indicated in Figure 4. *Expansions* of the (010) and (110) sigma planes in ferrierite yield the well known epididymite and feldspar double chains, respectively, illustrated in Figure 4. These double chains readily connect regions of undisturbed ferrierite type nets. In contrast to these expansions the contents of sigma planes in ferrierite can also be removed which gives rise to *sigma contractions*. The (010) sigma contraction amounts to an irregularity in the b repeat only, whereas the (110) sigma contraction also involves a shift by

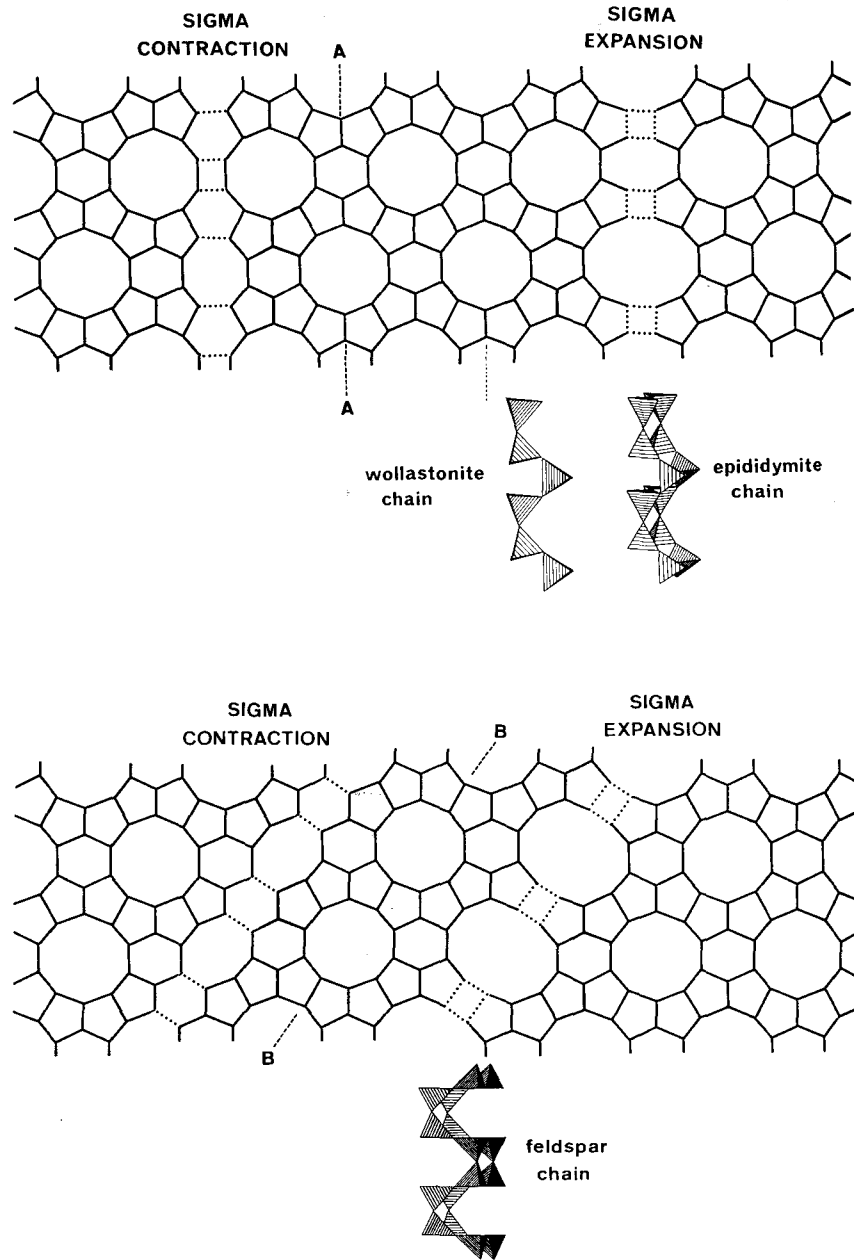


Fig. 4. Schematic crystal structures viewed along c illustrating the sigma fault models. Examples of sigma planes are marked A...A for $\sigma(010)$ and B...B for $\sigma(110)$. a): contraction and expansion faults for (010). b): contraction and expansion faults for (110). Chains formed parallel to c for the expansion faults are shown beneath the appropriate faults

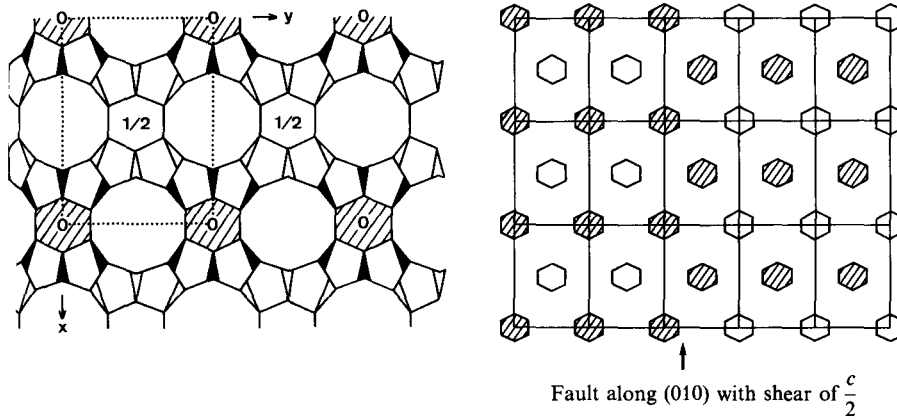


Fig. 5. Schematic crystal structures viewed along c for the order-disorder fault model. a): ferrierite structure represented by linked wollastonite chains. Black and white chains (∇ and \blacktriangledown) are displaced against each other by $c/2$. b): structure containing fault along (010) with shear of $c/2$

$c/2$. Geometric simulations based on DLS (Meier and Villiger, 1969; Baerlocher et al., 1978) confirmed that these sigma faults produce little or no local distortion of the ferrierite framework structure and are thus feasible.

These (010) and (110) sigma faults can indeed account for the diffuse streaks along $[010]^*$ and $[110]^*$ which have been repeatedly observed in SAD patterns. Only the $0\eta l$ patterns with continuous η streaks for l odd and sharp reflections for l even (observed in a few instances and shown in Fig. 3b) cannot be explained in terms of these faults.

This latter type of diffraction pattern (Fig. 3b) can be attributed to an additional mode of intergrowth. To describe the associated fault the ferrierite structure is conveniently considered as consisting of wollastonite chains (see insert in Fig. 4) oriented parallel c . The entire framework structure of ferrierite can be built from wollastonite chains. As is indicated in Figure 5a these chains are arranged in columns of six forming the stacks of 6-rings in the structure. Adjacent columns of 6 wollastonite chains are displaced by $c/2$ in the undisturbed ferrierite structure. Model considerations supplemented by DLS calculations showed that adjacent columns need not be displaced along $[001]$. A single undisplaced column would produce a linear fault in the ferrierite structure. 2-dimensional faults along (010), (110) etc. can be produced readily as indicated for (010) in Figure 5b. The superposition structure (Dornberger-Schiff and Dunitz, 1965) derived by superimposing the arrangement in Figure 5b with itself shifted by $c/2$ is fully ordered and the fault has vanished. Possible streaking $h\eta l$ with η continuous would thus be extinct for $l=2n$ as was observed occasionally (Fig. 3b). There is distinct evidence therefore for these conservative OD type faults to occur in ferrierite in addition to the nonconservative sigma faults.

Concluding remarks

The concept of sigma expansion and contraction faults is by no means limited to ferrierite only. Further studies will have to show how abundant these structural defects really are.

Wollastonite chains are not only frequent constituents of zeolite framework but are conceivably the most frequent chain-type building units of these structures. (Examples include mordenite, dachiardite, epistilbite, ferrierite, bikitaite, offretite, mazzite and Linde L). A large number of OD structures can be postulated on this basis.

Acknowledgements. Special thanks are due to Rudy W. Tschernich for providing us with samples of ferrierite for our investigations. We are indebted to Dr. H.-U. Nissen for letting us use the electron microscopy facilities of the Laboratorium für Festkörperphysik der ETH. This work was financially supported by the Swiss National Science Foundation.

References

- Baerlocher, Ch., Hepp, A., Meier, W. M.: DLS-76, a program for the simulation of crystal structures by geometric refinement. Institute of Crystallography and Petrography, ETH, Zurich. 124 pp. (1978)
- Bursill, L. A., Thomas, J. M., Rao, K. J.: Stability of zeolites under electron irradiation and imaging of heavy cations in silicates. *Nature* **289**, 157–158 (1981)
- Cartlidge, S., Wessicken, R., Nissen, H.-U.: Electron microscopy study of zeolite ZK-14, a synthetic chabazite. *Phys. Chem. Minerals* **9**, 139–145 (1983)
- Dornberger-Schiff, K., Dunitz, J.: Pseudo-orthorhombic diffraction patterns and OD structures. *Acta Crystallogr.* **19**, 471–472 (1965)
- Gramlich-Meier, R., Gramlich V., Meier, W. M.: The crystal structure of the monoclinic variety of ferrierite. *Am. Mineral.* (submitted)
- Hirsch, E. H.: Stability of zeolites under electron irradiation. *Nature* **293**, 759 (1981)
- Meier, W. M.: Zeolite structures. In: *Molecular sieves*, Society of Chemical Industry Special Publication. p. 10–25 (1968)
- Meier, W. M., Olson, D. H.: Atlas of Zeolite Structure Types. Special Publication by the Structure Commission of the International Zeolite Association, 99 pp. (1978)
- Meier, W. M., Villiger, H.: Die Methode der Abstandsverfeinerung zur Bestimmung der Atomkoordinaten idealisierter Gerüststrukturen. *Z. Kristallogr.* **129**, 411–423 (1969)
- Regis, A. J.: Occurrences of ferrierite in altered pyroclastics in central Nevada. *Geological Society of America Abstracts with Programs*, **2**, 661 (1970)
- Sheppard, R. A., Gude, A. J.: Guide to selected zeolite deposits in eastern Oregon, southwestern Idaho and northwestern Nevada. Field trip excursion guide for 6th International Conference on Zeolites, Reno, NV. 59 pp. (1983)
- Sherman, J. D., Bennett, J. M.: Framework structures related to the zeolite mordenite. *Adv. Chem. Ser.* **121**, 52–65 (1973)
- Shoemaker, D. P., Robson, H. E., Broussard, L.: The 'sigma transformation' interrelating certain known and hypothetical structures. *Proc. 3rd Int. Conf. on Molecular Sieves*, Zurich. p. 138–143 (1973)
- Thomas, J. M., Millward, G. R., Ramadas, S., Audier, M.: New approaches to the structural characterization of zeolites: High resolution electron microscopy and optical diffractometry. In: *Intrazeolite chemistry* (G. D. Stucky and F. G. Dwyer, eds.). American Chemical Society Symposium Series **218**, 181–198 (1983)
- Vaughan, P. A.: The crystal structure of the zeolite ferrierite. *Acta Crystallogr.* **21**, p. 983–990 (1966)
- Wise, W. S., Tschernich, R. W.: Chemical composition of ferrierite. *Am. Mineral.* **61**, 60–66 (1976)